

On the need to use steady-state or *operando* techniques to investigate reaction mechanisms: An in situ DRIFTS and SSITKA-based study example

Daniele Tibiletti, Alexandre Goguet, David Reid, Frederic C. Meunier*, Robbie Burch

CenTACat, School of Chemistry, Queen's University Belfast, Belfast BT9 5AG, Northern Ireland, UK

Available online 27 December 2005

Abstract

The nature of the surface species formed at the surface of 2 wt.% Pt/CeO₂ catalyst during the forward water-gas-shift (WGS, CO + H₂O → CO₂ + H₂) and the reverse reaction (RWGS) were essentially identical. More, the surface concentration of formate, carbonate and carbonyl species was similar in each case. The presence of well-resolved IR bands allowed an unequivocal relative quantitative analysis of each species, avoiding the use of the carboxylate stretching region (1600–1200 cm⁻¹). However, the quantitative analysis in the case of an isotopic study was complicated due to the overlapping of the various isotope bands, yet this problem could be overcome by integrating the high-wavenumber part of the bands. The reactivity of the surface species formed under RWGS conditions was followed under two different gaseous streams. Firstly, the reactivity of these intermediates were followed under an inert gas (i.e., Ar), in which case carbonates were essentially stable and less reactive than formates. Secondly, the reactivity of the same surface species was followed when switching to the corresponding ¹³C-labelled feed (i.e., ¹³CO₂ + H₂), in which case carbonates were exchanged significantly faster than formates. While carbonates species have been reported as reaction intermediate under reaction conditions, the increased stability or surface poisoning by these carbonates in the absence of reaction mixture was highlighted. Ultimately, this work re-emphasises the need to use steady-state conditions if the true *operando* reactivity of the adsorbates and structure of the solid are to be determined.

© 2005 Elsevier B.V. All rights reserved.

Keywords: *Operando*; In situ; Isotope; SSITKA; DRIFTS; FTIR; Spectroscopy; Water-gas-shift; Formate; Carbonate; Carbonyl; Surface species; IR band integration

1. Introduction

The interest in in situ techniques has been recently re-ignited by the introduction of the “*operando*” terminology, which somewhat stresses the need to use relevant feed conditions while carrying out simultaneously one or more spectroscopic analyses of the catalyst and/or surface adsorbates [1–7]. While many in situ or *operando* techniques are now routinely combined by many laboratories, it is surprising that the simultaneous utilisation of the steady-state isotopic transient kinetic analysis (SSITKA) technique and a spectroscopy has remained very limited. A pioneering work in the field was that carried out by Chuang et al. [8], who applied the SSITKA technique for the simultaneous analysis of reactor effluent and

of adsorbed species by in situ transmission FTIR spectroscopy during the study of CO methanation [9] and the hydroformylation of ethane [10]. Since, most other SSITKA investigations have only been concerned with the analysis of the gas-phase reactor effluent, which by itself provides already a number of valuable insights into reaction mechanisms [11–14]. Recently, Meunier et al. [15] and Jacobs et al. [16] have reported a combined analysis of the exchange of the species both at the surface of the catalyst and in the gas-phase during SSITKA investigation relating the water-gas-shift (WGS, Eq. (1)) reaction.



These authors used the combination of SSITKA and in situ IR to try to unravel the complex reaction pathway of the WGS reaction over noble metal supported on ceria, which are promising catalysts for the low temperature WGS needed for

* Corresponding author. Tel.: +44 28 90 974420; fax: +44 28 90 382117.
E-mail address: f.meunier@qub.ac.uk (F.C. Meunier).

the production CO-free hydrogen [17–30]. Various reaction mechanisms have been proposed regarding this reaction, some of which involved surface formate and/or carbonate species [19,31,28,32–35]. The reactivity and stability of the surface species observed over WGS catalysts are particularly intricate. Gorte et al. [26] investigated by diffuse reflectance FT-IR (DRIFT) the reactivity of surface species and noted that carbonates were stable on the reduced ceria but were easily decomposed by re-oxidation in either O₂ or H₂O. These authors proposed that the carbonates probably acted as a poison and limited the rate at which the ceria could be re-oxidized. Flytzani-Stephanopoulos et al. [36] proposed that the formation of ceria hydroxycarbonate was the main reason for the deactivation of Au-ceria catalysts, while Thompson et al. [37] proposed species reported as formate/carbonates. Farrauto et al. [38] and Meunier et al. [15] recently proposed that surface carbonates is a reaction intermediate normally decomposing to CO₂(g), but that an over-reduction of the support could lead to a strengthening of the carbonate bond, resulting in a self-poisoning of the catalyst by one of the reaction product [39]. Note that this latest view would nicely combine in one scheme a series of items relating to the deactivation, i.e., carbonate, catalyst over-reduction and reducing/oxidising nature of the reaction feed.

The conclusions of many of the IR studies were partly based on the observation of the surface species typically obtained under WGS reaction conditions and the decomposition/ reactivity of these species in vacuum or atypical feed gases [19,26,31,33]. Our laboratory has recently shown that the reactivity of carbonates and other surface species formed over Pt/CeO₂ during the reverse WGS (RWGS) reaction was strongly dependent on the experimental procedure used [40], and the data reported here complete this earlier preliminary report. The reactivity of the surface species formed under reverse water-gas-shift (RWGS) conditions (i.e., feed containing CO₂ and H₂), for which similar surface reactions as those occurring during the WGS are expected, based on the principle of microscopic reversibility. A particular attention is given to the method of integration of the IR bands of the species present at the surface of the sample. A key observation is the sensitivity of the key intermediates to changes in the reaction conditions, and the consequent risk of arriving at an incorrect mechanism. The implications of these observations are discussed with respect to the various reaction mechanisms that have been proposed for these reactions.

2. Experimental

The catalyst used in this study was a 2% Pt/CeO₂ provided by Johnson Matthey. The specific surface area, measured by the BET method on a Micromeritics ASAP 2010, was 180 m² g⁻¹. The Pt dispersion, measured by H₂ chemisorption on a Micromeritics Autochem 2910 at 193 K to minimize potential spillover of H₂ onto the support [41], was 17%. The purity of the gases used (i.e., H₂, He, CO₂, Ar, supplied by BOC) was higher than 99.95%. The ¹³CO₂ was 99% pure (supplied by Cambridge Isotope Laboratories Inc).

The experimental set-up consisted of an in situ high temperature diffuse reflectance IR cell (from Spectra-Tech[®]) fitted with ZnSe windows. The ceramic reactor used in the DRIFT cell was that supplied by the manufacturer, i.e., without any further modifications. The cell was connected to the feed gas cylinders through low volume stainless-steel lines. The gas flows were controlled by Aera mass flow controllers, which were regularly calibrated. A four-way valve was used to allow a fast switching between two reaction feeds, when appropriate. The DRIFTS cell was located in a Bruker Equinox 55 spectrometer, operating at a resolution of 4 cm⁻¹.

The amount of 2% Pt/CeO₂ catalyst used was always 30 ± 5 mg (particle diameter < 150 μm). Prior to any measurement, the sample was reduced in situ for 1 h at 573 K in a 50% H₂/Ar mixture at a total flow of 40 ml min⁻¹. Note that the seal between the reactor and the holder was not perfect and some of the feed gas was by-passing the catalyst. After the reduction step, the cell was purged with He and the temperature of the reactor was set to the desired value. The reaction mixture, i.e., 1% ¹²CO₂ + 4% H₂ in Ar, was then introduced at a total flow rate of 100 ml min⁻¹.

Steady-state conditions, as far as the nature and concentration of surface species measured by DRIFTS are concerned, was reached in less than 30 min. The assignment of the IR bands and the integration of the integration method are described in the results section. The IR data were reported as log 1/*R*, with *R* = *I*/*I*₀, where *R* is the sample reflectance, *I*₀ is the intensity measured on the sample after reduction in hydrogen and *I* that measured under reaction condition. The function log 1/*R* gives a better linear representation of the band intensity against sample surface coverage than that given by the Kubelka–Munk function for strongly absorbing media such as our Pt/CeO₂ [42].

3. Results

3.1. Assignment of IR bands

The typical in situ DRIFT spectra obtained over the 2% Pt/CeO₂ under reverse and forward WGS reaction feeds were essentially identical (Fig. 1). The assignment of the DRIFTS bands has been described in details elsewhere [43,44]. The bands at 2947 and 2841 cm⁻¹ are associated with the combination band δ(C–H) + ν_s(OCO) and ν(C–H) of a bidentate formate species located on the ceria, respectively [43,44]. The bands in the region 1600–1200 cm⁻¹ were mostly due to the stretching vibration modes (symmetric and anti-symmetric) of the O–C–O group of free carboxylate, formate and carbonate species. Due to the complexity of this band structure, the deconvolution and interpretation of this region was not attempted. The complex band structure between 2100 and 1900 cm⁻¹ is related to Pt-bound carbonyl species. The high-frequency side of the band (centred around 2070 cm⁻¹) is associated with linearly bound CO, probably on a distribution of heterogeneous adsorption sites, whereas the lower frequency side of the band may be related to bridged carbonyl species [45]. The bands in the 900–800 cm⁻¹ region are associated with

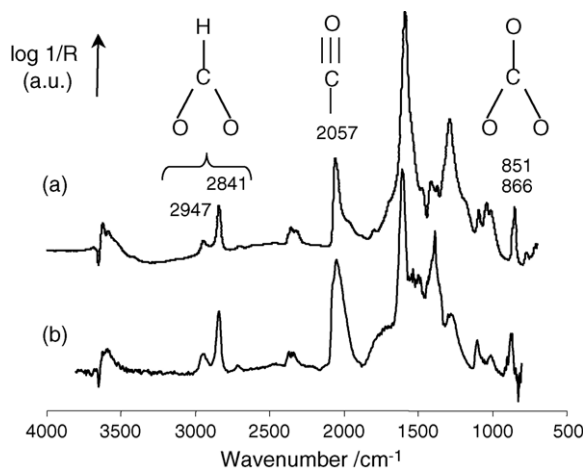


Fig. 1. Typical in situ DRIFT spectra obtained over a 2% Pt/CeO₂ at steady-state conditions under (a) a RWGS feed: 1% CO₂ + 4% H₂ in Ar at 498 K and (b) a WGS feed: 1% CO + 10% H₂O in Ar at 473 K.

the out-of-plane vibration of carbonate species. At least two carbonate bands were observed (i.e., non-resolved bands at 866 and 851 cm⁻¹), related to different adsorption sites (probably mostly on the support) and/or bonding mode to the surface. While it is possible that some formates and carbonates may also be located on the metal, it is likely that the corresponding IR bands were swamped by that of the corresponding species located over the high surface area support.

3.2. Evolution of the bands formed under RWGS following a switch to Ar

Figs. 2–4 show the DRIFT spectra of the catalyst (pre-exposed to reverse-WGS feed) at 498 K at various stages of the isothermal desorption in an Ar flow. The surface formates were markedly reactive in this inert atmosphere (Fig. 2) and completely desorbed or decomposed; e.g., the bands at 2947 and 2841 cm⁻¹ vanished (without peak shifting) in ca. 1 h (Fig. 2f). The evolution of the carbonyls band was more complex (Fig. 3). The high-wavenumber part of the carbonyl band was quickly removed and the peak gradually shifted from 2057 cm⁻¹ at steady-state conditions in RWGS mixture

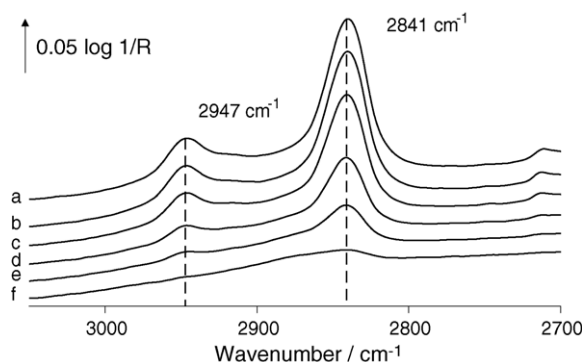


Fig. 2. In situ DRIFT spectra of the surface formate species formed over a 2% Pt/CeO₂ catalyst at 498 K (a) at steady state in 1% ¹²CO₂ + 4% H₂ in Ar, and after (b) 1 min, (c) 2 min, (d) 5 min, (e) 10 min and (f) 60 min under Ar at 498 K.

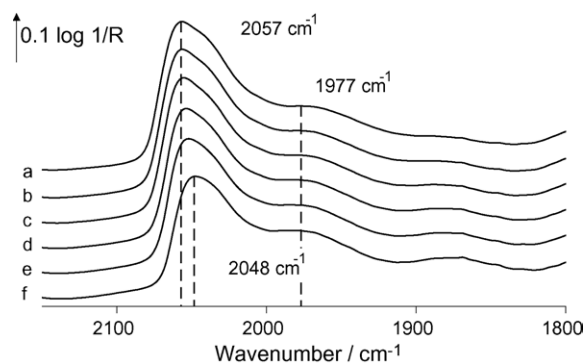


Fig. 3. In situ DRIFT spectra of the carbonyl species formed over a 2% Pt/CeO₂ catalyst at 498 K (a) at steady state in 1% ¹²CO₂ + 4% H₂ in Ar, and after (b) 1 min, (c) 2 min, (d) 5 min, (e) 10 min and (f) 60 min under Ar at 498 K.

(Fig. 3a) to 2048 cm⁻¹ after 60 min in Ar (Fig. 3f). The species absorbing at 1970 cm⁻¹ showed no significant change; this band was possibly related to bridged CO(ads) or some Pt–H stretching vibration (Fig. 3). The changes on the carbonate bands were minor (Fig. 4). The low-wavenumber frequencies part of the peak (i.e., 851 cm⁻¹) slowly decreased in intensity, gradually blue-shifting to 854 cm⁻¹ after 60 min in Ar (Fig. 4f). The other carbonate species (i.e., 866 cm⁻¹) increased in intensity to a minor extent.

3.3. Evolution of the bands formed under RWGS following a switch to a labelled feed

Fig. 5 shows the evolution of the formate bands after switching the unlabelled RWGS mixture to the corresponding ¹³C-labelled feed. The intensity of the formate band at 2947 cm⁻¹ (i.e., combination $\delta(\text{C-H}) + \nu_s(\text{OCO})$) decreased, while a new band appeared at 2916 cm⁻¹ ($\Delta\nu = 31$ cm⁻¹). Simultaneously, the other formate band at 2841 cm⁻¹ (i.e., $\nu(\text{C-H})$) shifted to 2825 cm⁻¹. In this case the red-shift was lower, $\Delta\nu = 16$ cm⁻¹, and the bands of the two formate isotopes partly overlapped. The ¹²C-containing formates were completely replaced by the ¹³C-containing species after ca. 45 min (Fig. 5f).

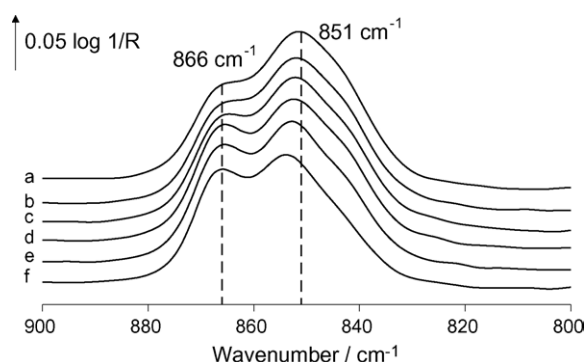


Fig. 4. In situ DRIFT spectra of the surface carbonate species formed over a 2% Pt/CeO₂ catalyst at 498 K (a) at steady state in 1% ¹²CO₂ + 4% H₂ in Ar, and after (b) 1 min, (c) 2 min, (d) 5 min, (e) 10 min and (f) 60 min under Ar at 498 K.

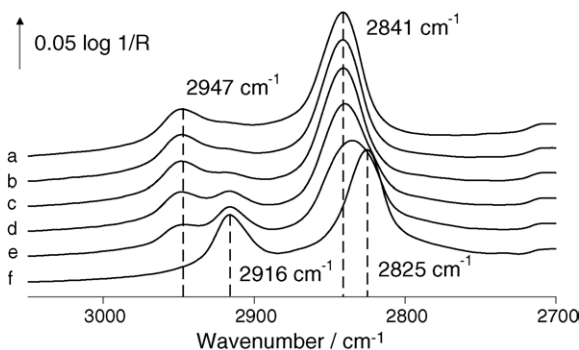


Fig. 5. In situ DRIFT spectra of the surface formate species formed over a 2% Pt-CeO₂ catalyst at 498 K (a) at steady state in 1% ¹²CO₂ + 4% H₂ in Ar, and after (b) 1, (c) 2, (d) 5, (e) 10 and (f) 90 additional minutes under 1% ¹³CO₂ + 4% H₂ in Ar at 498 K.

The ¹²C-carbonyl band at 2057 cm⁻¹ was replaced by a ¹³C-species absorbing at 2010 cm⁻¹ upon exposure to the labelled RWGS mixture (Fig. 6). The $\Delta\nu$ was equal to 49 cm⁻¹, as usually observed for the exchange of carbonyls [46,47]. Ortelli et al. [48] used the method of the reduced masses in order to calculate the theoretical shift of the carbonyl band, obtaining the following equation:

$$\text{Wavenumber } (^{13}\text{C}-\text{O}) = 0.9778 \times \text{Wavenumber } (^{12}\text{C}-\text{O})$$

Employing this formula, the carbonyl peak located at 2058 cm⁻¹ would be expected to shift to 2012 cm⁻¹, in good agreement with the experimental result obtained (i.e., 2010 cm⁻¹). The low-wavenumber feature (shoulder at ca. 1977 cm⁻¹) was removed and a new feature at 1904 cm⁻¹ was also formed. The large shift observed ($\Delta\nu = 73$ cm⁻¹) suggests that these species may not be related. The replacement of the ¹²C-containing species was completed in about 15 min.

The isotopic exchange of the surface carbonates readily took place when the labelled RWGS mixture was introduced (Fig. 7). The high-wavenumber part of the band disappeared completely in ca. 2 min (Fig. 7c) and subsequently yield a negative component at 862 cm⁻¹ (Fig. 7f). The negative band observed at 862 cm⁻¹ indicated that some of the carbonate species that were present on the sample after the pre-reduction were readily

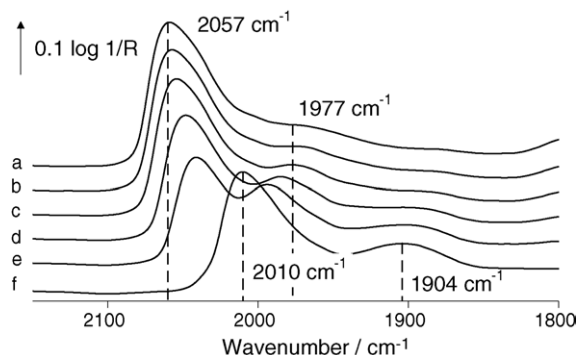


Fig. 6. In situ DRIFT spectra of the carbonyl species formed over a 2% Pt/CeO₂ catalyst at 498 K (a) at steady state in 1% ¹²CO₂ + 4% H₂ in Ar, and after (b) 1, (c) 2, (d) 5, (e) 10 and (f) 90 additional minutes under 1% ¹³CO₂ + 4% H₂ in Ar at 498 K.

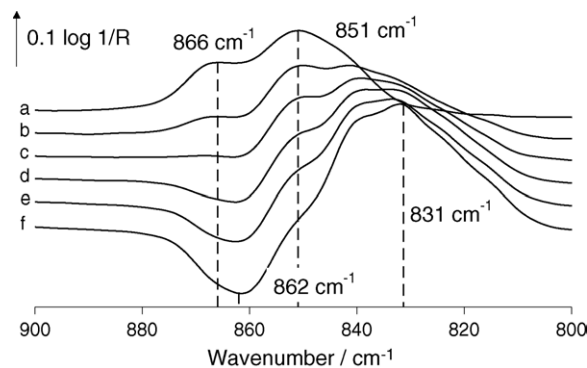


Fig. 7. In situ DRIFT spectra of the surface carbonate species formed over a 2% Pt/CeO₂ catalyst at 498 K (a) at steady state in 1% ¹²CO₂ + 4% H₂ in Ar, and after (b) 1, (c) 2, (d) 5, (e) 10 and (f) 90 additional minutes under 1% ¹³CO₂ + 4% H₂ in Ar at 498 K.

exchanged in RWGS conditions. A new band at 831 cm⁻¹ appeared, which can be assigned to the out-of-plane bending vibration of ¹³C-containing carbonates [49]. The ¹²C-¹³C isotopic wavenumber shift of an out-of-plane carbonate vibration mode is expected to be of a factor 0.97 [50]. The ¹²C-containing carbonate band at 851 cm⁻¹ probably fully overlapped with the band of the ¹³C-containing carbonate derived from the 866 cm⁻¹ ¹²C-containing species expected at $866 \times 0.97 = 840$ cm⁻¹. Note that the low-wavenumber side of the ¹³C-containing band is related to the low-wavenumber side of the original ¹²C-containing band, and that an identical exchange rate as that measured on the high-wavenumber side was observed (see next section). The replacement of the ¹²C-containing species was essentially complete in about 10 min (Fig. 7).

3.4. Integration of the IR bands

The wavenumber regions selected in Figs. 2–4 were unequivocally related to one type of surface species. The IR bands of these species typically exhibited a red-shift when the ¹²C isotope was replaced with the heavier ¹³C isotope (Figs. 5–7). Unfortunately, the shift in frequency was not sufficient to allow a complete resolution of the ¹²C and ¹³C-IR bands. A number of methods were attempted to quantify the relative concentrations of the various surface species of interest, including a full deconvolution by Gaussian or Lorentzian curves of the IR bands, without any satisfactory outcome. The integration of the high-wavenumber part of the bands, which corresponded to the ¹²C-containing species, gave the most satisfactory results. The wavenumber limits that were used for the quantification of the concentrations of the ¹²C-containing surface species of interest were as follows (the area of a given band was measured with the OPUS software, using a single-point baseline), all values being in cm⁻¹.

Formate: 2954–2944 (single-point baseline at 3050).

Carbonyl: 2110–2050 (single-point baseline at 2150).

Carbonate: 900–865 (single-point baseline at 795).

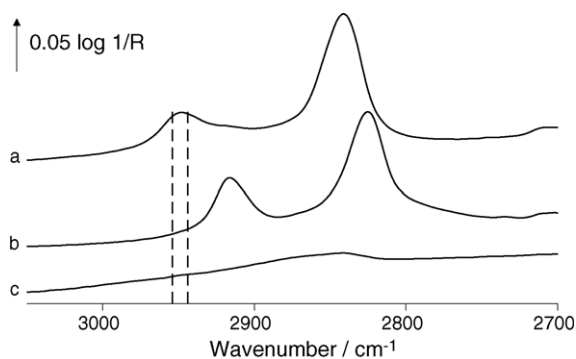


Fig. 8. Integration region (vertical lines, see text for limit details) of the DRIFT spectra of the surface formate species formed over a 2% Pt/CeO₂ catalyst at 498 K (a) at steady state in 1% ¹²CO₂ + 4% H₂ in Ar, (b) at steady state in 1% ¹³CO₂ + 4% H₂ in Ar at 498 K and (c) after 60 min under Ar at 498 K after exposure to the ¹²C-containing RWGS mixture. The signal of the reduced catalyst at the same temperature under Ar was used as background.

The limits of the integration of the formate band are shown in Fig. 8. The relative variation of the formate band intensity integrated within these (narrow) limits and that obtained by integrating the full band (3000–2775 cm⁻¹) during the desorption in Ar (Fig. 2) are essentially identical (Fig. 9). The integration limits of the carbonyl and carbonate bands are shown in Figs. 10 and 11. No such validation could be obtained for the carbonyl and carbonates bands, as those were hardly reactive under Ar.

The equivalence between the ¹²C-related high-wavenumber region and the ¹³C-related low-wavenumber region for the quantification of the exchange rate of the carbonate band is shown in Fig. 12. The high-wavenumber part of the out-of-plane carbonate vibration was integrated as described above, while the low-wavenumber region was integrated between 825–800 cm⁻¹, using a single-point baseline at 800 cm⁻¹. Note that the complement to unity (i.e., 1-¹³C-related signal) is shown in the latter case for the sake of comparison. These data clearly show that the same exchange profile was obtained by using either method.

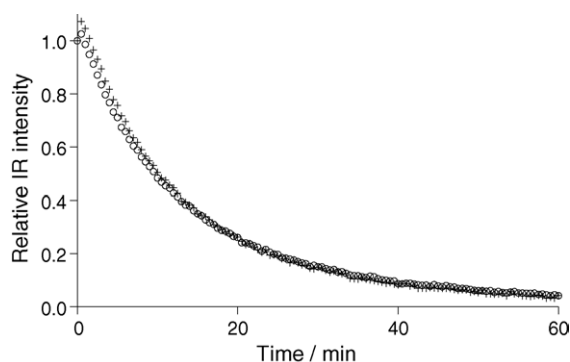


Fig. 9. Relative intensity of the IR formate bands as a function of time on stream in Ar, following steady-state state in 1% ¹²CO₂ + 4% H₂ integrating (○) the full peak and (+) the limited high-wavenumber region as indicated in the text. *T* = 498 K.

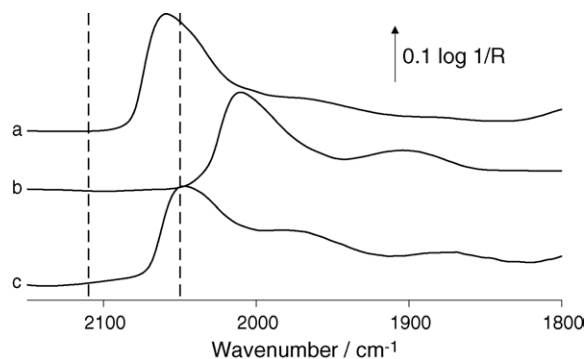


Fig. 10. Integration region (vertical lines, see text for limit details) of the DRIFT spectra of the surface carbonyl species formed over a 2% Pt/CeO₂ catalyst at 498 K (a) at steady state in 1% ¹²CO₂ + 4% H₂ in Ar, (b) at steady state in 1% ¹³CO₂ + 4% H₂ in Ar at 498 K and (c) after 60 min under Ar at 498 K after exposure to the ¹²C-containing RWGS mixture. The signal of the reduced catalyst at the same temperature under Ar was used as background.

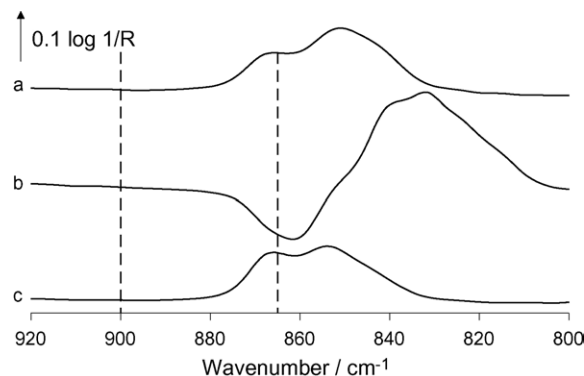


Fig. 11. Integration region (vertical lines, see text for limit details) of the DRIFT spectra of the surface carbonate species formed over a 2% Pt/CeO₂ catalyst at 498 K (a) at steady state in 1% ¹²CO₂ + 4% H₂ in Ar, (b) at steady state in 1% ¹³CO₂ + 4% H₂ in Ar at 498 K and (c) after 60 min under Ar at 498 K after exposure to the ¹²C-containing RWGS mixture. The signal of the reduced catalyst at the same temperature under Ar was used as background.

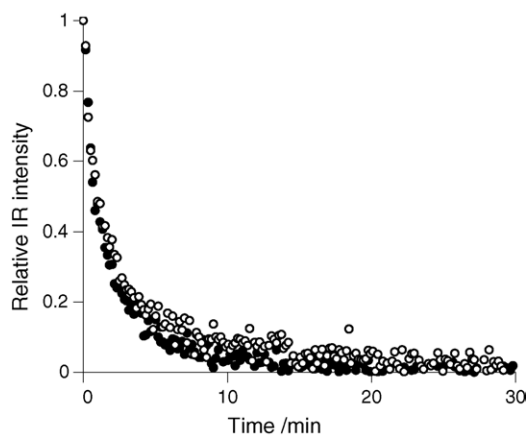


Fig. 12. Relative evolution of the intensity of the out-of-plane carbonate band as a function of time on stream in 1% ¹³CO₂ + 4% H₂, following steady-state state in 1% ¹²CO₂ + 4% H₂. The integration was carried out on (○) the ¹²C-related high-wavenumber region and (●) the ¹³C-related low-wavenumber region of the band as indicated in the text. Note that the complement to unity (i.e., 1-¹³C-related signal) is shown in the latter case, for the sake of comparison. *T* = 498 K.

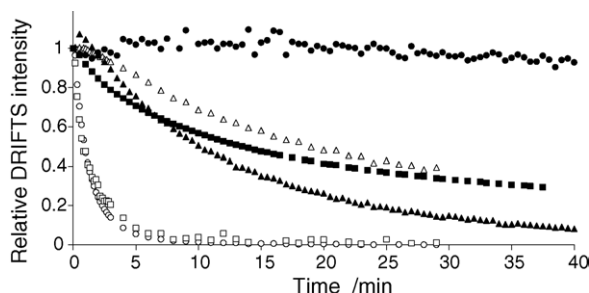


Fig. 13. Relative intensity of the IR bands of the formate (\blacktriangle , \triangle), carbonyl (\blacksquare , \square) and carbonate (\bullet , \circ) species as a function of time on stream in Ar (solid symbols) and under RWGS stream containing $^{13}\text{CO}_2$ (open symbols). The sample was at steady-state state in 1% $^{12}\text{CO}_2$ + 4% H_2 and $T = 498\text{ K}$ before switching to either Ar or the $^{13}\text{CO}_2$ -containing feed.

3.5. Evolution of the bands formed under RWGS following a switch to Ar or the labelled feed

The variation of the intensity of the formate, carbonate and carbonyl species following a switch from steady-state under the RWGS feed to Ar (Fig. 13, solid symbols) and to the corresponding labelled feed (Fig. 13, open symbols) showed dramatic differences.

When switching to Ar (Figs. 2 and 13), the intensity of the formate band rapidly decreased to zero. A 50% loss in signal intensity was observed after ca. 10 min. The carbonyl signal initially decreased (Fig. 13) at a similar rate as that of the formates, but a significant fraction of these species was still actually present after 1 h (Fig. 3). The chosen integration limits on the high-wavenumber side of the band was clearly not representative of the whole collection of CO(ads) present. The intensity of the carbonate bands remained essentially constant with time, probably indicating that the small fraction of the species removed at 851 cm^{-1} band was quantitatively being converted to that at 866 cm^{-1} (Fig. 4).

When switching to the labelled feed (Fig. 13, open symbol), a complete exchange of both the carbonyl and carbonate species could be obtained in less than 10 min, that is, faster than the exchange time of the formates. It is also surprising to note that the rate of isotopic exchange of the formates was slower than that of desorption/decomposition of these same species under Ar (i.e., time for 50% exchange and desorption/decomposition: 20 and 10 min, respectively).

The relevance of the integration method was tested comparing the kinetics of isotopic exchange for the forward ($^{12}\text{CO}_2 \rightarrow ^{13}\text{CO}_2$) and reverse ($^{13}\text{CO}_2 \rightarrow ^{12}\text{CO}_2$) isotopic switch (data not shown). The normalised band intensities for the forward and reverse switches were plotted versus time and led to identical profiles, both for the formate and carbonate species. However, in the case of the carbonyl species significantly different shapes were obtained for the forward and the reverse switch.

4. Discussion

4.1. Carbonyl signal

The IR signal corresponding to the carbonyls is complex as: (1) a distribution of heterogeneous adsorption sites can be expected over supported noble metal particles and (2) the occurrence of dipole–dipole (i.e., lateral) interactions take places at the typical high surface coverage observed under our reaction conditions [51].

The two phenomena mentioned above have to be taken into account when studying the evolution of the carbonyl band profile with time. The morphology and crystallite size of the metal particles results in the formation of several different adsorption sites (i.e., terrace, step, hollow) [52,53]. The frequency of the CO vibration is sensitive to the number of metallic atoms to which it is bonded, as well as to the coordination number of the metal [54]. The CO bonded to low energy sites (rising band at high-frequency) are expected to be exchanged first [55,56]. The carbonyl species corresponding to the high-wavenumber range investigated ($2110\text{--}2050\text{ cm}^{-1}$) should be the most reactive fraction of carbonyls adsorbed on the catalyst surface. However, there is a substantial interaction between accommodated carbonyls and adsorbing species from the gas-phase, resulting in high mobility of the CO(ads) on the metal surface. Yoshinobu and Kawai [53] proposed an indirect adsorption mechanism in which transient mobile molecules interacted with already accommodated molecules (collision on the surface) inducing migration of CO on the metal surface (the lateral translational energy of the incoming molecule would be used to overcome the energy barrier between different sites).

The second phenomenon of importance is the coverage-dependent band shifting and it is given by the combination of two primary components: the chemical shift and the dipole–dipole shift. The chemical shift (or static dipole) is due to changes in the electron distribution between CO and the metal as the surface density of adsorbed CO molecules increases. For CO–Pt system, the chemical shift has been reported to be circa 10 cm^{-1} [55–58]. In the present study, the chemical composition at the metal surface was only changed during the experiment under Ar, and any chemical shift can be ruled out during the isotope exchange. The dipole–dipole shift (or dynamic dipole) occurs due to the interaction between adjacent vibrating dipoles (electrodynamical interaction) on the catalyst surface. The coupling between identical molecules produces an upward shift in the vibrational frequency of a few tens of cm^{-1} , typically less than 20 cm^{-1} [54]. The coupling between dissimilar molecules (i.e., molecules bonded to different adsorption sites or molecules with different isotopic composition) produces a more dramatic effect. Typically, for the CO–Pt system, the dipole shift has been reported to be circa $10\text{--}20\text{ cm}^{-1}$ [55–58]. Moreover, the band shift is associated with a characteristic “transfer of intensity” from modes at low frequency to their higher frequency counterpart [59,54,60,61] and to changing in the molar absorption coefficient. Another phenomenon associated with the band shifting is the formation

of CO islands, which increases the dipole–dipole interactions [61,62].

The coverage-dependent band shifting (mainly due to the dipole–dipole interaction) and the intensity borrowing effect (either from step sites to terrace sites or from isotopes) caused distortion of the DRIFT spectrum of the carbonyl species. Therefore, the carbonyl band cannot be used as such for the quantification of a relative CO population at specific sites [56]. The rapid disappearance of the high-wavenumber fraction of the carbonyl band (Figs. 3 and 6) could be due to a number of processes as described above.

The singleton of the ^{12}C carbonyl species, measured at low $^{12}\text{CO}_2(\text{ads})$ concentration in $^{13}\text{CO}_2(\text{ads})$ during the isotope exchange, was ca. 2040 cm^{-1} . Typically this band is associated with CO linearly adsorbed on defect sites [54]. Under steady-state conditions (4% H_2 + 1% $^{12}\text{CO}_2$) the carbonyl band was centred at 2058 cm^{-1} (Fig. 6). The band shifting was due to the increase of the dipole–dipole interaction as the surface density of $\text{Pt}-^{12}\text{CO}$ species increased. The same behaviour was observed for the formation of the $\text{Pt}-^{13}\text{CO}$ band during the $^{12}\text{CO}_2 \rightarrow ^{13}\text{CO}_2$ switch (Fig. 6). First a band at about 1980 cm^{-1} formed (the precise location of this band was not possible because it overlapped with the low frequency part of the ^{12}C -containing carbonyl band). Afterwards the band shifted to 2009 cm^{-1} . Once again the upward shift was due to the intensification of the dipole–dipole interaction as the density of the $\text{Pt}-^{13}\text{CO}$ species increased.

It is worth highlighting that in both cases (^{12}C - and ^{13}C -containing carbonyls) the band shift could be estimated at $20\text{--}30\text{ cm}^{-1}$. In the literature, the band shift due to the dipole–dipole interaction is reported to be equal to $10\text{--}20\text{ cm}^{-1}$. The higher value of the shift reported in this study is likely to be due to the combination of the dipole–dipole shift and the shift due to the presence of a variety of adsorption sites on the Pt surface. In conclusion, the observed variation of the carbonyl intensity (Fig. 13) is qualitative and a rigorous calibration of the intensity versus surface coverage (both for a single or combined isotopes) would be necessary to obtain more reliable kinetic information.

4.2. Carbonate and formate species signals

No such intensity transfer effects are known for the IR signal carbonate and formate species supported on oxides. The data reported in Fig. 9 shows that the integration of the high-wavenumber fraction of the formate IR band is equivalent to that of the whole band. The data reported in Fig. 12 show that the carbonate band could be integrated either on the ^{12}C or ^{13}C side of the band. This also suggests that all carbonates were exchanged at a similar rate, despite the fact that those displayed a range of vibration wavenumbers (e.g., 866 and 851 cm^{-1}).

Our data clearly show that *operando* studies are necessary in order to investigate the true reactivity pattern of surface species during the RWGS over noble metal-promoted ceria. An experiment in which the RWGS reaction intermediates are allowed to accumulate on the catalyst surface and then

react or decompose in an inert atmosphere, leads to the conclusion that formates are the most reactive species, while carbonates are essentially stable (Fig. 13, solid symbols). However, when the reaction intermediates are allowed to react or decompose under steady-state conditions (studied by isotopic switching techniques) it is found that carbonate species are the most reactive surface compounds (Fig. 13, open symbols).

Other experiments have shown that the carbonate species are readily desorbed following the addition of O_2 to the inert purge gas [26,39]. This suggests that one of the main origins for the difference in the reactivity of surface species with respect to the reaction feed may be related to the average oxidation state of the ceria. With respect to this point, while our reaction feed (i.e., 1% CO_2 + 4% H_2) was globally reducing, the actual steady-state oxidation state of the ceria under RWGS conditions will depend of the relative rate of reduction by H_2 (and the CO formed) and of oxidation by CO_2 (and the water formed). These observations emphasise the fact that different experimental conditions affect the oxidation state of ceria and, as a consequence, the likelihood of a redox or a non-redox (e.g., formate-based) reaction mechanism will change. The increase stability of carbonates (main surface reaction intermediate [15]) over reduced ceria could also explain a deactivation of noble metal-promoted ceria catalyst during WGS when the latter becomes “over-reduced” and the possible remedy proposed by several authors by periodic oxidation treatments [38] or even the introduction of traces of O_2 in the WGS stream [63].

5. Conclusions

The nature and surface concentration of the species formed over a Pt-CeO_2 under WGS and RWGS feed are essentially identical in the conditions reported here. Formate, carbonate and carbonyl species were clearly identified. The integration of well-resolved IR bands allowed an unequivocal relative quantitative analysis of each species, avoiding the use of the carboxylate stretching region ($1600\text{--}1200\text{ cm}^{-1}$). The utilisation of the high-wavenumber part of a formate band was shown to be equivalent to the quantification of the whole band. The utilisation of the ^{12}C -related high-wavenumber side of the out-of-plane bending vibration mode of the carbonates was shown to be equivalent to that of the ^{13}C -related low-wavenumber side. The quantitative analysis of the carbonyl signals was not possible here and would required detailed calibration of the intensity versus Pt coverage.

The reactivity of these intermediates were followed under an inert gas (i.e., Ar), in which case carbonates were essentially stable and less reactive than formates. The reactivity of the same surface species was also followed under the corresponding ^{13}C -labelled feed, in which case the carbonates were exchanged significantly faster than formates. The data reported here clearly show the need to use *operando* or steady-state techniques (such as steady-state isotopic kinetic analysis, SSITKA) to determine the reactivity of surface species in actual operating conditions.

Acknowledgements

Johnson Matthey is acknowledged for supplying the catalyst. This work was supported by the EPSRC, under the CARMAC project. We gratefully thank one of the referees for his comments about IR band assignments.

References

- [1] H. Topsøe, *J. Catal.* 216 (2003) 155.
- [2] H. Topsøe, J.A. Dumesic, H. Topsøe, *J. Catal.* 151 (1995) 241.
- [3] T.C. Schilke, I.A. Fisher, A.T. Bell, *J. Catal.* 184 (1999) 144.
- [4] B.M. Weckhuysen, *Phys. Chem. Chem. Phys.* 5 (2003) 4351.
- [5] A. Bruckner, *Catal. Rev. Sci. Eng.* 45 (2003) 97.
- [6] M.A. Banares, *Catal. Today* 100 (2005) 71.
- [7] T. Lesage, C. Verrier, P. Bazin, J. Saussey, S. Malo, C. Hedouin, G. Blanchard, M. Daturi, *Top. Catal.* 30 (2004) 31.
- [8] S.S.C. Chuang, M.A. Brundage, M.W. Balakos, G. Srinivas, *Appl. Spectrosc.* 49 (1995) 1151.
- [9] M.W. Balakos, S.S.C. Chuang, G. Srinivas, *J. Catal.* 140 (1993) 281.
- [10] S.A. Hedrick, S.S.C. Chuang, M.A. Brundage, *J. Catal.* 185 (1999) 73.
- [11] D.M. Stockwell, J.S. Chung, C.O. Bennett, *J. Catal.* 112 (1988) 135.
- [12] A.M. Efstathiou, T. Chafik, D. Bianchi, C.O. Bennett, *J. Catal.* 147 (1994) 24.
- [13] M. Agnelli, H.M. Swaan, D. Marquez-Alvarez, G.A. Martin, C. Mirodatos, *J. Catal.* 175 (1998) 117.
- [14] T. Chafik, A.M. Efstathiou, X.E. Verykios, *J. Phys. Chem. B* 101 (1997) 7968.
- [15] A. Goguet, D. Tibiletti, F.C. Meunier, J.P. Breen, R. Burch, *J. Phys. Chem. B* 108 (2004) 20240.
- [16] G. Jacobs, B. Davis, *Appl. Catal. A: Gen.* 284 (2005) 31.
- [17] B.I. Whittington, C.J. Jiang, D.L. Trimm, *Catal. Today* 26 (1995) 41.
- [18] J. Barbier Jr., D. Duprez, *Appl. Catal. B: Environ.* 4 (1994) 105.
- [19] T. Shido, Y. Iwasawa, *J. Catal.* 141 (1993) 71.
- [20] J.T. Kummer, *J. Phys. Chem.* 90 (1986) 4747.
- [21] E.C. Su, W.G. Rothschild, *J. Catal.* 99 (1986) 506.
- [22] R.K. Hertz, J.A. Sell, *J. Catal.* 94 (1985) 166.
- [23] K.C. Taylor, Automobile catalytic converters, in: J.R. Anderson, M. Boudard (Eds.), *Catalysis: Science and Technology*, vol. 5, Springer, Berlin, 1984.
- [24] T. Bunluesin, R.J. Gorte, G.W. Graham, *Appl. Catal. B: Environ.* 15 (1998) 107.
- [25] J.M. Zalc, V. Sokolyskii, D.G. Löffler, *J. Catal.* 206 (2002) 169.
- [26] S. Hilaire, X. Wang, T. Luo, R.J. Gorte, J. Wagner, *Appl. Catal. A: Gen.* 215 (2001) 271.
- [27] X. Wang, R.J. Gorte, *Catal. Lett.* 73 (2001) 15.
- [28] Q. Fu, A. Weber, M. Flytzani-Stephanopoulos, *Catal. Lett.* 77 (2001) 87.
- [29] T. Luo, R.J. Gorte, *Catal. Lett.* 85 (2003) 139.
- [30] X. Wang, R.J. Gorte, J.P. Wagner, *J. Catal.* 212 (2002) 225.
- [31] T. Shido, Y. Iwasawa, *J. Catal.* 136 (1992) 493.
- [32] Y. Li, Q. Fu, M. Flytzani-Stephanopoulos, *Appl. Catal. B: Environ.* 27 (2000) 179.
- [33] G. Jacobs, L. Williams, U. Graham, D. Sparks, B.H. Davis, *J. Phys. Chem. B* 107 (2003) 10398.
- [34] G. Jacobs, L. Williams, U. Graham, D. Sparks, G. Thomas, B.H. Davis, *Appl. Catal. A: Gen.* 252 (2003) 107.
- [35] G. Jacobs, E. Chenu, P.M. Patterson, L. Williams, D. Sparks, G. Thomas, B.H. Davis, *Appl. Catal. A: Gen.* 258 (2004) 203.
- [36] Q. Fu, W. Deng, H. Saltsburg, M. Flytzani-Stephanopoulos, *Appl. Catal. B: Environ.* 56 (2005) 57.
- [37] C.H. Kim, L.T. Thompson, *J. Catal.* 230 (2005) 66.
- [38] X. Liu, W. Ruettinger, X. Xu, R. Farrauto, *Appl. Catal. B: Environ.* 56 (2005) 69.
- [39] F.C. Meunier, D. Tibiletti, A. Goguet, D. Reid, R. Burch, *Appl. Catal. A: Gen.* 289 (2005) 104.
- [40] D. Tibiletti, A. Goguet, F.C. Meunier, J.P. Breen, R. Burch, *Chem. Commun.* (2004) 1636.
- [41] S. Bernal, F.J. Botana, J.J. Calvino, M.A. Cauqui, G.A. Jobacho, J.M. Pintado, J.M. Rodriguez-Izquierdo, *J. Phys. Chem.* 97 (1993) 4118.
- [42] J.M. Olinger, P.R. Griffiths, *Anal. Chem.* 60 (1988) 2427.
- [43] G. Busca, J. Lamotte, J.C. Lavalley, V. Lorenzelli, *J. Am. Chem. Soc.* 109 (1987) 5197.
- [44] C. Binet, M. Daturi, J.C. Lavalley, *Catal. Today* 50 (1999) 207.
- [45] P. Bazin, O. Saur, J.C. Lavalley, M. Daturi, G. Blanchard, *Phys. Chem. Chem. Phys.* 7 (2005) 187.
- [46] C. Mihut, C. Descorme, D. Duprez, M.D. Amiridis, *J. Catal.* 212 (2002) 125.
- [47] D. Roth, G.J. Lewis, X.D. Jiang, L.F. Dahl, M.J. Weaver, *J. Phys. Chem.* 96 (1992) 7219.
- [48] E.E. Ortel, J.M. Weigel, A. Wokaun, *Catal. Lett.* 54 (1998) 41.
- [49] C. Binet, A. Badri, J.C. Lavalley, *J. Phys. Chem.* 98 (1994) 6392.
- [50] M.E. Bottcher, M.E. Gehlken, *Appl. Spectrosc.* 51 (1997) 130.
- [51] A. Bourane, O. Dulaurent, D. Bianchi, *J. Catal.* 196 (2000) 115.
- [52] C. Elmasides, X.E. Verykios, *J. Catal.* 203 (2001) 477.
- [53] J. Yoshinobu, M. Kawai, *Surf. Sci.* 363 (1996) 105.
- [54] P. Hollins, *Surf. Sci. Rep.* 16 (1992) 51.
- [55] P.T. Fanson, W.N. Delgass, J. Lauterbach, *J. Catal.* 204 (2001) 35.
- [56] C.S. Kim, W.J. Tornquist, C. Korzeniewski, *J. Chem. Phys.* 101 (1994) 9113.
- [57] P.C. Welch, P.S.W. Mills, C. Mason, P. Hollins, *J. Electron. Spectrosc. Relat. Phenom.* 64–65 (1993) 151.
- [58] J. Lauterbach, R.W. Boyle, M. Schick, W.J. Mitchell, B. Meng, W.H. Weinberg, *Surf. Sci.* 366 (1996) 228.
- [59] M.W. Severson, C. Stuhlmann, I. Villegas, M.J. Weaver, *J. Chem. Phys.* 103 (1995) 9832.
- [60] S.G. Fox, V.M. Browne, P. Hollins, *J. Electron. Spectrosc. Relat. Phenom.* 54 (1990) 749.
- [61] M.Y. Smirnov, G.W. Graham, *Catal. Lett.* 72 (2001) 39.
- [62] P.B. Wells, *Appl. Catal.* 18 (1985) 259.
- [63] W. Deng, M. Flytzani-Stephanopoulos, 19th NAM, Philadelphia, May 2005 (abstract O-305).